THE JOURNAL OF BIOLOGICAL CHEMISTRY
Vol. 275, No. 49, Issue of December 8, pp. 38337–38346, 2000

Printed in U.S.A.

Escherichia coli MutL Loads DNA Helicase II onto DNA*

Received for publication, July 14, 2000, and in revised form, August 28, 2000
Published, JBC Papers in Press, September 12, 2000, DOI 10.1074/jbc.M006268200

Leah E. Mechanic‡§¶, Brenda A. Frankel¶‖, and Steven W. Matson‡‡§§**

*From the Departments of ‡Biochemistry and Biophysics, ‖Chemistry, and **Biology, the §Protein Engineering and Molecular Genetics Training Program, and the ‡‡Curriculum in Genetics and Molecular Biology, University of North Carolina, Chapel Hill, North Carolina 27599*

Previous studies have shown that MutL physically interacts with UvrD (DNA helicase II) (Hall, M. C., Jordan, J. R., and Matson, S. W. (1998) *EMBO J.* 17, 1535–1541) and dramatically stimulates the unwinding reaction catalyzed by UvrD in the presence and absence of the other protein components of the methyl-directed mismatch repair pathway (Yamaguchi, M., Dao, V., and Modrich, P. (1998) *J. Biol. Chem.* 273, 9197–9201). The mechanism of this stimulation was investigated using DNA binding assays, single-turnover helicase assays, and unwinding assays involving long duplex DNA substrates. The results indicate that MutL binds DNA and loads UvrD onto the DNA substrate. The interaction between MutL and DNA and that between MutL and UvrD are both important for stimulation of UvrD-catalyzed unwinding. MutL does not clamp UvrD onto the substrate; and therefore, the processivity of unwinding is not increased in the presence of MutL. The implications of these results are discussed, and models are presented for the mechanism of MutL stimulation as well as for the role of MutL as a master coordinator in the methyl-directed mismatch repair pathway.

Mismatch repair is the primary mechanism for repair of replication errors in *Escherichia coli* (1–3). The mismatch repair machinery also prevents recombination between highly divergent DNA sequences (4, 5). Thus, an active mismatch repair system ensures the precision of chromosomal replication and maintains genomic stability (for reviews, see Refs. 1–3). Consistent with this idea, defects in mismatch repair genes in human cells have been linked to genomic instability and hereditary colon cancer, underscoring the importance of this repair pathway (6–9).

The sequence of biochemical reactions that define the mismatch repair pathway has been well described in *E. coli*, and the proteins responsible for each step are known (for reviews, see Refs. 1–3). Mismatch recognition is accomplished by a MutS dimer (10, 11). MutL, also a dimer, then binds the MutS·DNA complex (12), and the DNA is looped out in an active search for the nearest d(GATC) methylation site either 5′ or 3′ of the mismatch (12, 13). Once found, the complex stimulates MutH to generate a nick on the unmethylated (or nascent) strand at the hemimethylated d(GATC) site (14–16). DNA helicase II and the appropriate exonuclease then excise the error-containing DNA (17, 18), beginning at the nick and continuing past the mismatch (18). The single-stranded DNA (ssDNA)[1] gap is filled by DNA polymerase III, and DNA ligase seals the remaining nick (19).

Importantly, the mismatch repair reaction pathway has bidirectional capability. The nick is generated at the d(GATC) site located closest to the mismatch and therefore could exist on either side of the mismatch (18). However, DNA helicase II unwinds DNA with a specific 3′ to 5′ polarity (20). As a result, helicase II must be loaded on the appropriate DNA strand to ensure unwinding toward the mismatch. It is also important to note that the d(GATC) site nearest an error may be >1 kilobase away (19).

The precise biochemical activity associated with the MutL protein has been a matter of debate for several years. Some groups have demonstrated that MutL binds to both ssDNA and double-stranded DNA (21, 22), whereas others have reported that MutL does not bind DNA (23). It is now clear that MutL catalyzes a weak ATPase reaction and that this activity is required for mismatch repair (21, 24, 25). In addition, MutL stimulates the biochemical activities of MutS, MutH, and helicase II (12, 13, 23, 24, 26–29), and several lines of evidence indicate there is a physical interaction between MutL and MutS (12, 13, 23), MutL and MutH, and MutL and helicase II (26, 27). Thus, MutL has been suggested to function as a master coordinator or molecular matchmaker in the mismatch repair pathway (1, 29, 30).

Of particular interest is the fact that MutL specifically stimulates the unwinding reaction catalyzed by DNA helicase II (the *uvrD* gene product) (27, 29). The unwinding activity of the Rep protein (40% identical to UvrD) is enhanced by MutL, but to a significantly lower extent (29). Moreover, on a nicked circular heteroduplex DNA substrate, MutL and MutS together activate UvrD-catalyzed unwinding, whereas there is no detectable enhancement of unwinding by Rep helicase (29). Thus, stimulation of the UvrD-catalyzed unwinding reaction by MutL is specific and likely due to a protein-protein interaction. This is consistent with data demonstrating a physical interaction between these two proteins (25, 26).

Little is known about the mechanism by which the UvrD-catalyzed unwinding reaction is enhanced by MutL. However, important details of the reaction have been described. For example, on a nicked circular molecule containing a mismatch, MutS, MutL, and UvrD initiate unwinding at the nick site and begin helix opening in the direction toward the mismatch. This reaction requires all three protein components and the presence of a mismatch (31). In addition, although MutL dramatically stimulates the unwinding rate by DNA helicase II, MutL

* This work was supported by National Institutes of Health Grant GM 33476 (to S. W. M.). The costs of publication of this article were defrayed in part by the payment of page charges. This article must therefore be hereby marked "*advertisement*" in accordance with 18 U.S.C. Section 1734 solely to indicate this fact.

¶ The first two authors contributed equally to this work.

§§ To whom correspondence should be addressed: Dept. of Biology, CB 3280, Coker Hall, University of North Carolina, Chapel Hill, NC 27599-3280. Tel.: 919-962-0005; Fax: 919-962-1625; E-mail: smatson@tbio.unc.edu.

[1] The abbreviations used are: ssDNA, single-stranded DNA; bp, base pair(s); AMP-PNP, adenosine5′-(β,γ-imino)triphosphate.

does not increase the ATP hydrolysis rate of helicase II (26).

The mechanism responsible for stimulation of UvrD-catalyzed unwinding by MutL has been investigated. The experiments described here support a model in which MutL loads UvrD onto the DNA substrate, increasing the rate of initiation. In addition, MutL-directed loading of UvrD is observed to be continuous. A model for methyl-directed mismatch repair is presented that incorporates the observed biochemical and physical interactions between MutL and UvrD.

EXPERIMENTAL PROCEDURES

Bacterial Strains and Plasmids—E. coli BL21 was from Novagen. GE1752Δ*mutS* (28) was constructed previously in this laboratory. Plasmids pET11d, pLysS, and pET3c were from Novagen. Plasmids pCYB2 and pLitmus28 were from New England Biolabs Inc. M13mp7 ssDNA was purified as described previously (32). Plasmid pCYB2-*mutL* (intein fusion construct) was constructed previously (28). The plasmid that expresses UvrD has been described (33).

Oligonucleotides and Enzymes—Restriction endonucleases, DNA polymerase I (large fragment), and T4 polynucleotide kinase were from New England Biolabs Inc. and were used as recommended by the supplier. The 48-base oligonucleotide 5′-GGAAAAATTAGTTTCTCT-TACTCTCTTTATGATATTTAAAAAAGCGGT-3′ was used in electrophoretic mobility shift assays and as a trap in some helicase assays.

Protein Purification—UvrD was purified as described previously (34). Purification of pCYB2-mUTL from BL21 was as described previously (26). This protein was used for nitrocellulose filter binding experiments.

Additional MutL was purified from a strain lacking MutS, GE1752Δ*mutS*. MutL was overexpressed prior to purification by growing GE1752Δ*mutS* containing pCYB2-*mutL* in 2× yeast-tryptone medium at 30 °C. Cells were grown to an absorbance of 1.0 (600 nm). Protein expression was induced by the addition of 0.5 mM isopropyl-β-D-thiogalactopyranoside.

For purification from GE1752Δ*mutS* containing pCYB2-*mutL*, 19.5 g of cells were harvested by centrifugation. pCYB2-*mutL* generates the MutL protein as an intein fusion. MutL was purified using a chitin column (Impact I system, New England Biolabs Inc.) according to the manufacturer's instructions. Protein was eluted with buffer containing 20 mM Tris-HCl (pH 8.0 at 25 °C), 10% (v/v) glycerol, and 0.1 mM EDTA supplemented with 0.2 M NaCl and 30 mM dithiothreitol. Pooled fractions were diluted with buffer A (20 mM Tris-HCl (pH 7.5 at 25 °C), 10% (v/v) glycerol, and 0.1 mM EDTA) to a conductivity equivalent to that of buffer A + 0.1 M NaCl. The pool was loaded onto a 10-ml DEAE-Sephadex column (2.7-cm internal diameter; Sigma) that had been equilibrated with buffer A + 0.1 M NaCl. Protein was eluted from the column with a linear gradient of 0.1–0.6 M NaCl in buffer A. Protein eluted at a conductivity equivalent to that of buffer A + 0.13 M NaCl. Pooled fractions (8 ml) were concentrated by solution absorption with polyethylene glycol 20,000. Fractions were placed in a dialysis bag with a molecular weight cutoff of 3500. The dialysis bag was covered with polyethylene glycol 20,000. Then, 3 ml of concentrated protein material were extensively dialyzed into MutL storage buffer (20 mM Tris-HCl (pH 7.5 at 25 °C), 50% (v/v) glycerol, 0.2 M NaCl, 0.1 mM EDTA, and 1 mM 2-mercaptoethanol).

The concentration of helicase II was determined using the published extinction coefficient of 1.29 ml mg^{-1} cm^{-1} (35). The concentration of MutL was determined using the Bradford protein assay (Bio-Rad) with bovine serum albumin as a standard.

DNA Substrates—A 148-bp blunt duplex DNA fragment was produced by digestion of pLitmus28 with *Xba*I and *Pvu*II and purified from an agarose gel using Geneclean (Bio 101, Inc.). The purified DNA fragment was radioactively labeled by filling in the *Xba*I site with [α-^{32}P]dCTP, dTTP, dATP, and dGTP using DNA polymerase I (large fragment). After phenol/chloroform extraction, the DNA fragment was separated from unincorporated nucleotides using a Sephadex G-50 column (Sigma). The concentration of the final product was estimated assuming an 80% yield.

The 750-bp blunt duplex DNA fragment was prepared by digestion of pLitmus28 with *Dra*I, followed by treatment with calf intestinal phosphatase (Roche Molecular Biochemicals) to produce 5′-OH. The fragment was isolated from an agarose gel using Geneclean and was subsequently labeled with [γ-^{32}P]ATP and T4 polynucleotide kinase. The DNA fragment was purified as described above using an A-5m column (Bio-Rad). The concentration was estimated as indicated above.

The 20-bp partial duplex substrate used in single-turnover assays was prepared by labeling the single-stranded 20-mer with [γ-^{32}P]ATP and T4 polynucleotide kinase. The labeled 20-mer was mixed in annealing buffer (50 mM NaCl, 10 mM Tris-HCl (pH 7.5 at 22 °C), and 1 mM $MgCl_2$) with M13mp7 ssDNA at a 1:1 molar ratio. The annealing mixture was heated at 95 °C for 5 min, followed by successive 20-min incubations at 65, 42, and 22 °C. The 92-bp partial duplex used in single-turnover assays was annealed as described above prior to labeling with [α-^{32}P]dCTP as described previously (36). Following labeling and annealing, DNA substrates were diluted to 100 μl in 100 mM NaCl, 10 mM Tris-HCl (pH 7.5 at 25 °C), and 1 mM EDTA and phenol/chloroform-extracted. Unincorporated nucleotides were removed using a Sephadex G-50 spin column as described (37). Concentrations were estimated assuming an 85% yield. The 851- and 92-bp partial duplex substrates used in standard helicase and nitrocellulose filter binding assays were prepared as described previously (36).

Nitrocellulose Filter Binding—The binding of UvrD, MutL, and UvrD + MutL to DNA was evaluated by measuring the retention of a [^{32}P]DNA ligand on nitrocellulose filters as described previously (38, 39). Experiments were done using a ^{32}P-labeled 90-mer (0.4 nM molecules; 36 nM nucleotide phosphate) or a 92-bp partial duplex substrate (0.17 nM molecules; 1.2 μM nucleotide phosphate). Reaction mixtures contained 25 mM Tris-HCl (pH 7.5 at 22 °C), 3 mM $MgCl_2$, 20 mM NaCl, 5 mM 2-mercaptoethanol, and 50 μg/ml bovine serum albumin (reaction buffer). These experiments contained the indicated concentrations of UvrD and/or MutL. Proteins were diluted in helicase II storage buffer (20 mM Tris-HCl (pH 8.3 at 22 °C), 0.2 M NaCl, 25 mM 2-mercaptoethanol, 50% (v/v) glycerol, 1 mM EDTA, and 0.5 mM EGTA).

Equilibrium binding experiments were done in 20-μl reactions. UvrD and MutL were premixed. Reaction tubes were prewarmed for 30 s at 37 °C and initiated by the addition of premixed protein. Reactions were incubated at 37 °C for 10 min and diluted with 1 ml of reaction buffer without bovine serum albumin immediately before filtration. The entire reaction was then filtered.

Reactions were filtered using the double-filter technique (40) over nitrocellulose membranes (Millipore Corp.) and NA45-DEAE filters (Schleicher & Schüll). Nitrocellulose filters (38) and DEAE filters (40) were prepared as described and rinsed with 1 ml of reaction buffer with bovine serum albumin prior to application of the reaction mixtures. Reactions were filtered at a flow rate of ~2 ml/min. Filters were washed two times with 1 ml of reaction buffer and dried for liquid scintillation counting. Total radioactivity was determined for each titration or time point as the sum of radioactivity on the nitrocellulose filter and the DEAE filter. Background values, determined from nitrocellulose filters of no-protein controls, were typically <1% of the total counts. Relative macroscopic K_D values were calculated from equilibrium binding data by fitting the equation for a rectangular hyperbola to the data. Data fitting was done using the nonlinear least-squares technique and SigmaPlot (Jandel Scientific). Error values in binding constants were generated by SigmaPlot.

Gel Mobility Shift Assays—Gel shift reaction mixtures (20 μl) contained 25 mM Tris-HCl (pH 7.5 at 22 °C), 3 mM $MgCl_2$, 20 mM NaCl, 5 mM 2-mercaptoethanol, 0.7 nM ^{32}P-labeled 48-base oligonucleotide (32 nM nucleotide phosphate), and 1 mM AMP-PNP. Proteins were diluted in helicase II storage buffer, premixed, and incubated on ice before initiation by the addition of the other reaction components. All reactions were incubated for 20 min on ice, followed by the addition of 5 μl of 75% (v/v) glycerol to all reaction tubes and loading dyes to the control tube that contained only the oligonucleotide. Glycerol or dyes did not alter the apparent migration of the ssDNA oligonucleotide (data not shown).

Samples were immediately loaded onto an 8% polyacrylamide gel (67:1 cross-linking ratio) containing 50 mM Tris, 50 mM borate, and 2.5 mM EDTA. Samples were electrophoresed at constant voltage (8 V/cm) until the bromphenol blue marker had migrated to ~1 inch from the bottom of the gel. Results were visualized using a Storm 840 PhosphorImager (Molecular Dynamics, Inc.).

Helicase Assays—Standard helicase reaction mixtures (290 μl) contained 25 mM Tris-HCl (pH 7.5 at 22 °C), 3 mM $MgCl_2$, 20 mM NaCl, 5 mM 2-mercaptoethanol, 50 μg/ml bovine serum albumin, and the indicated [^{32}P]DNA substrate (0.28 nM 750-bp blunt duplex, 0.4 nM 851-bp partial duplex, or 0.17 nM 92-bp partial duplex). Proteins were diluted in helicase II storage buffer, and protein was premixed (either UvrD and storage buffer or UvrD and MutL) prior to combination with the other reaction components. Reactions were prewarmed at 37 °C prior to initiation with ATP (to 3 mM), and incubation was continued at 37 °C. Following initiation, 20-μl samples were withdrawn at the indicated times and quenched by combining with 10 μl of stop solution (37.5% glycerol, 50 mM EDTA, and 0.5% each xylene cyanol and bromphenol blue). Reaction products were resolved on 8% nondenaturing polyacryl-

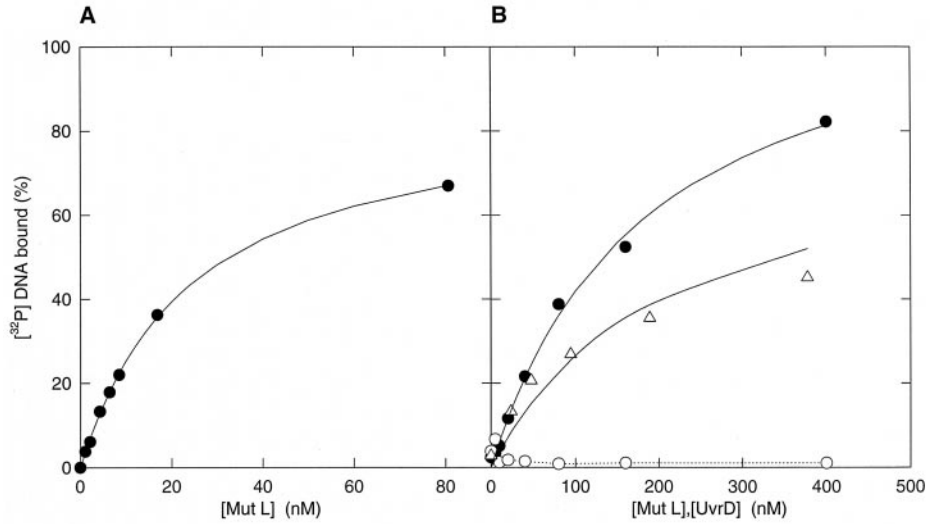

FIG. 1. **DNA-binding properties of MutL.** Nitrocellulose filter binding experiments were performed as described under "Experimental Procedures" using the indicated concentrations of purified protein. *A*, retention of a [^{32}P]DNA 92-bp partial duplex substrate by MutL (●) in the absence of nucleotide. The equation for a rectangular hyperbola was fit to the data (*solid line*). *B*, binding of UvrD (△) and MutL (○) to a [^{32}P]DNA 90-mer in the absence of nucleotide. The binding of MutL (●) in the presence of AMP-PNP is also shown. The equation for a rectangular hyperbola was fit to data from the binding of UvrD (△) and MutL (●) in the presence of AMP-PNP (*solid lines*). Data points from the binding of MutL (○) in the absence of nucleotide were connected (*dashed line*). Data represent the averages of multiple independent trials.

amide gels. Results were visualized and quantified using a Storm 840 PhosphorImager and ImageQuant software (Molecular Dynamics, Inc.). Data obtained for the initial 10 min of the reaction, avoiding points where the concentration of DNA substrate becomes limiting, were fit to Equation 1 from Amaratunga and Lohman (41),

$$A(t) = A_b(1 - e^{(-k_b t)}) + v_{ss}t \quad \text{(Eq. 1)}$$

where $A(t)$ is the total amplitude or femtomoles unwound at time t, A_b is the amplitude of the burst phase, k_b is the rate constant for the burst phase, and v_{ss} is the steady-state rate of unwinding represented by the second phase of the curve (41). Values of kinetic constants were determined using the nonlinear least-squares technique and SigmaPlot. Error values were generated by SigmaPlot.

For the experiment shown in Fig. 6, the helicase reaction mixture was assembled as indicated for standard helicase assays with the 148-bp blunt duplex at a final concentration of 0.15 nM molecules. Reactions were performed at 22 °C. Reactions were incubated for 1 min at 22 °C prior to initiation of the unwinding reaction with ATP (to 3 mM) in a total reaction volume of 120 μl. After 30 s had elapsed, 1 μl of 0.5 mM 48-mer was added to the reaction mixture to trap free UvrD. Samples were withdrawn, quenched, and analyzed as indicated above.

In single-turnover helicase assays, reactions were assembled as described above with a final DNA substrate concentration of 1 nM. Unwinding reactions were incubated at 18 °C. Reactions were preincubated on ice for 10 min and at 18 °C for 4 min prior to initiation of unwinding with a mixture of ATP (to 3 mM) and 48-mer (to 8 μM) for a total reaction volume of 120 μl. Sample removal, quenching, and analysis were as indicated above.

RESULTS

MutL has been shown to dramatically stimulate the unwinding reaction catalyzed by UvrD as part of a reconstituted mismatch repair reaction and in a standard helicase assay lacking the other enzymes involved in mismatch repair (27, 29). However, the biochemical mechanism of this stimulation is not known. To further investigate this stimulation, MutL was purified to near homogeneity from a strain lacking the *mutS* gene (see "Experimental Procedures") (data not shown). This was done to avoid any complications that might arise from the presence of low level contamination by MutS. It should be noted that experiments performed with MutL purified from a Δ*uvrD* strain produced results similar to those produced by experiments performed with MutL purified from a Δ*mutS* strain (27) (data not shown).

MutL Binding to ssDNA and Partial Duplex DNA—Previous experiments reached contradictory conclusions regarding the ability of MutL to bind DNA (21–23). The binding of MutL to ssDNA or to a partial duplex DNA ligand was evaluated using a nitrocellulose filter binding assay (Fig. 1). MutL bound to the 92-bp partial duplex DNA with an apparent K_D of 25 nM (Fig. 1*A*, ●), but failed to bind ssDNA ([^{32}P]DNA 90-mer) in the absence of nucleotide at concentrations up to 400 nM (Fig. 1*B*, ○). The failure of MutL to bind to ssDNA in the absence of nucleotide was confirmed by electrophoretic mobility shift assay (data not shown). However, limited binding of MutL to ssDNA was observed in the presence of ATP (data not shown). More significant binding to the ssDNA oligonucleotide was apparent with the MutL protein in the presence of the poorly hydrolyzed ATP analog AMP-PNP (Fig. 1*B*, ●). The apparent K_D was 180 nM. Previous studies have demonstrated that MutL binds AMP-PNP with a greater affinity than ATP (24). Therefore, it is likely that the limited effect of ATP on ssDNA binding compared with the more significant effect of AMP-PNP is due to the greater binding affinity of MutL for AMP-PNP. It is also apparent that a MutL·ATP complex is competent to bind ssDNA. These experiments were repeated with other preparations of MutL, including MutL from a Δ*uvrD* strain, producing similar results (data not shown).

Under the same experimental conditions, in the absence of nucleotide cofactor, the binding of UvrD to the [^{32}P]DNA 90-mer was examined (Fig. 1*B*, △). The data for the binding of UvrD to the ssDNA 90-mer were poorly described by the equation for a rectangular hyperbola (unlike the binding of MutL in the presence of nucleotide), indicating that the binding of ssDNA by UvrD in the absence of nucleotide is more complicated than this simple saturation model. However, using the equation for a rectangular hyperbola to analyze the data, the apparent K_D for the interaction of UvrD with ssDNA was determined to be 200 nM. This estimation of the K_D for UvrD binding to ssDNA is likely an underestimate. Nonetheless, this value is consistent with the values reported previously for the binding of UvrD to ssDNA in the absence of nucleotide (38, 42).

MutL Enhances the ssDNA Binding of UvrD—The migration of a single-stranded [^{32}P]DNA 48-mer on a polyacrylamide gel was decreased by interaction with UvrD (Fig. 2, compare *lanes 1* and *6*). The smeared appearance of the DNA suggested that

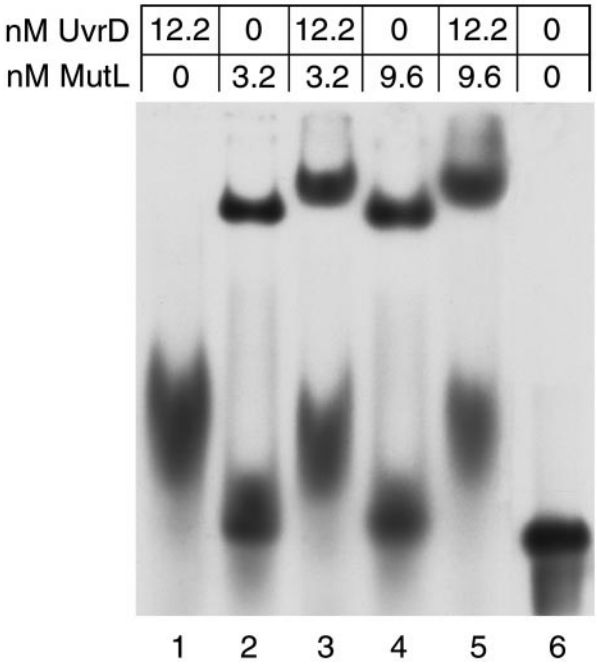

FIG. 2. **Electrophoretic mobility shift assays with MutL, UvrD, and UvrD + MutL.** Gel mobility shift assays were performed with a ^{32}P-labeled ssDNA 48-mer as detailed under "Experimental Procedures." The binding of the indicated concentrations of UvrD (*lane 1*), MutL (*lanes 2* and *4*), or UvrD + MutL (*lanes 3* and *5*) to the 48-mer is shown. The ^{32}P-labeled ssDNA 48-mer incubated in the absence of protein is shown in *lane 6*.

dissociation of the UvrD·48-mer complex occurred during electrophoresis. This was evident when protein·DNA complexes were transferred to nitrocellulose and probed using anti-UvrD antibodies. The anti-UvrD antibodies failed to react with the smeared DNA material, but recognized material that migrated more slowly on the gel, consistent with dissociation of UvrD from the DNA during electrophoresis (data not shown). The addition of 3.2 and 9.6 nM MutL also slowed the mobility of the ssDNA fragment and formed a distinct species with retarded mobility (*lanes 2* and *4*). Thus, MutL was able to stably interact with the ssDNA 48-mer in the presence of AMP-PNP, consistent with the results obtained in the nitrocellulose filter binding assays.

When 12.2 nM UvrD was incubated together with 3.2 or 9.6 nM MutL, a supershifted species was observed migrating more slowly than the species due to either MutL alone or UvrD alone (Fig. 2, compare *lanes 2* and *4* with *lanes 3* and *5*). The supershifted species was observed only in the presence of MutL + UvrD and was not apparent in the presence of either MutL or UvrD alone even when the concentration of MutL was increased from 3.2 to 9.6 nM (*lanes 2* and *4*) or higher (data not shown) or when the concentration of UvrD was increased (data not shown). It is likely that the supershifted species is due to the specific interaction between MutL and UvrD, and not to UvrD and MutL independently binding to the ssDNA for the following reasons. MutL and UvrD physically interact both *in vitro* (in the absence of DNA) and *in vivo* (25, 26). In addition, in the presence of MutL + UvrD, there was a complete absence of the DNA species associated with MutL alone (compare *lanes 2* with *lanes 3* and *5*), indicating that MutL prefers to bind to UvrD·DNA. Moreover, it had been observed by Western blotting that UvrD was associated only with the supershifted species, and not with the smeared species (*lane 1*) (data not shown). Thus, UvrD alone dissociated from DNA during the course of the electrophoresis. However, after the addition of MutL, a distinct supershifted species was observed, indicating that MutL strengthens the interaction of UvrD with DNA or that the MutL·UvrD·DNA complex has a greater affinity for ssDNA than UvrD alone.

The data presented above suggest that MutL increases the binding of UvrD to DNA. Both the affinity of UvrD for ssDNA and the stability of the complex were improved in the presence of MutL. Therefore, MutL could stimulate UvrD-catalyzed unwinding either by loading the helicase onto the DNA substrate or by clamping the helicase onto the DNA and acting to increase its processivity.

Single-turnover Unwinding of a 20-bp Partial Duplex—To address the idea that MutL enhances the UvrD-catalyzed unwinding of duplex DNA by loading UvrD onto the DNA, we performed a series of single-turnover experiments using a 20-bp partial duplex substrate. Either UvrD or UvrD + MutL were preincubated with the 20-bp partial duplex substrate to allow binding, and the reaction was initiated by the addition of a mixture of ATP and a ssDNA 48-mer trap. The addition of the trap eliminated further binding of UvrD to the partial duplex substrate such that any unwinding observed was the result of UvrD bound to the 20-bp partial duplex substrate prior to initiation of the reaction. Given that the processivity of UvrD has been observed to be 40–50 base pairs (43), it is expected that once UvrD initiates unwinding, it will complete the unwinding of the 20-bp region. Stimulation of unwinding by MutL is therefore interpreted as evidence for preloading of helicase II.

Fig. 3*A* shows the results of these experiments. It should be noted that MutL alone did not catalyze unwinding of the 20-bp partial duplex substrate (data not shown). In the absence of MutL, UvrD (20 nM) unwound <10% of the 20-bp partial duplex substrate. This is consistent with the K_D for the binding of UvrD to a partial duplex substrate in the absence of nucleotide (38, 44). With increasing concentrations of MutL, the same concentration of UvrD was able to unwind increasing amounts of the substrate (up to 85% with 160 nM MutL). This result clearly illustrates that MutL enhances UvrD-catalyzed unwinding under single-turnover conditions, suggesting that MutL functions to load UvrD onto the DNA prior to initiation of unwinding.

The amplitudes of the curves shown in Fig. 3*A* were calculated using a modified form of Equation 1. Since the data from these experiments have only an exponential phase, the constant term was omitted from calculations. These calculated amplitudes were plotted as a function of MutL concentration (Fig. 3*B*), and a saturation curve was observed. Interestingly, the MutL concentration at which the amplitude was half its maximal value (40 ± 10 nM) corresponded closely to the apparent K_D (25 nM) for MutL binding to a partial duplex substrate (see Fig. 1*A*). This finding suggests that, although MutL and UvrD are known to physically interact (25, 26), stimulation of the UvrD-catalyzed unwinding reaction is also related to the ability of MutL to bind DNA. Since the fraction of the substrate unwound is directly related to the amount of UvrD productively pre-bound to DNA, it follows that MutL increases the affinity of UvrD for a partial duplex substrate. This effect was not directly measurable with nitrocellulose filter binding assays due to the ability of MutL to bind to a partial duplex DNA ligand in the absence of ATP (see Fig. 1*A*).

MutL Stimulates Unwinding Catalyzed by UvrD on Long Duplex DNA Substrates—The results from the DNA binding data and the single-turnover unwinding reactions suggest that MutL increases the affinity of UvrD for ssDNA and may increase the affinity of UvrD for single-stranded/double-stranded junctions. Therefore, MutL stimulates UvrD-catalyzed unwinding by loading UvrD onto the DNA substrate. Since load-

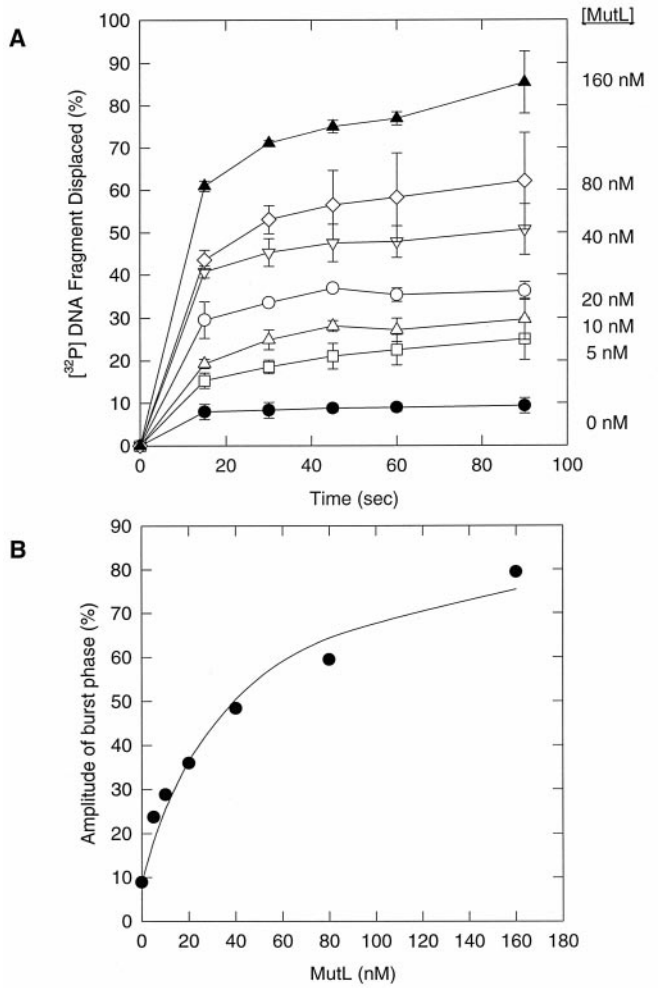

FIG. 3. **Single-turnover unwinding experiments with the 20-bp partial duplex substrate.** *A*, the unwinding activity of 20 nM UvrD alone (●) or 20 nM UvrD plus the indicated concentrations of MutL (5 nM (□), 10 nM △, 20 nM (○), 40 nM (▽), 80 nM (◇), and 160 nM (▲)) was measured as described under "Experimental Procedures." The fraction unwound was calculated for each protein concentration and time shown as described previously (38). Data represent the average of at least three independent experiments. *Error bars* are means ± S.D. *B*, Equation 1 was fit to the data in *A* to determine the amplitude of the burst phase (A_b) at each MutL concentration. Amplitude is plotted against nanomolar MutL. The equation for a rectangular hyperbola was fit to the data (*solid line*).

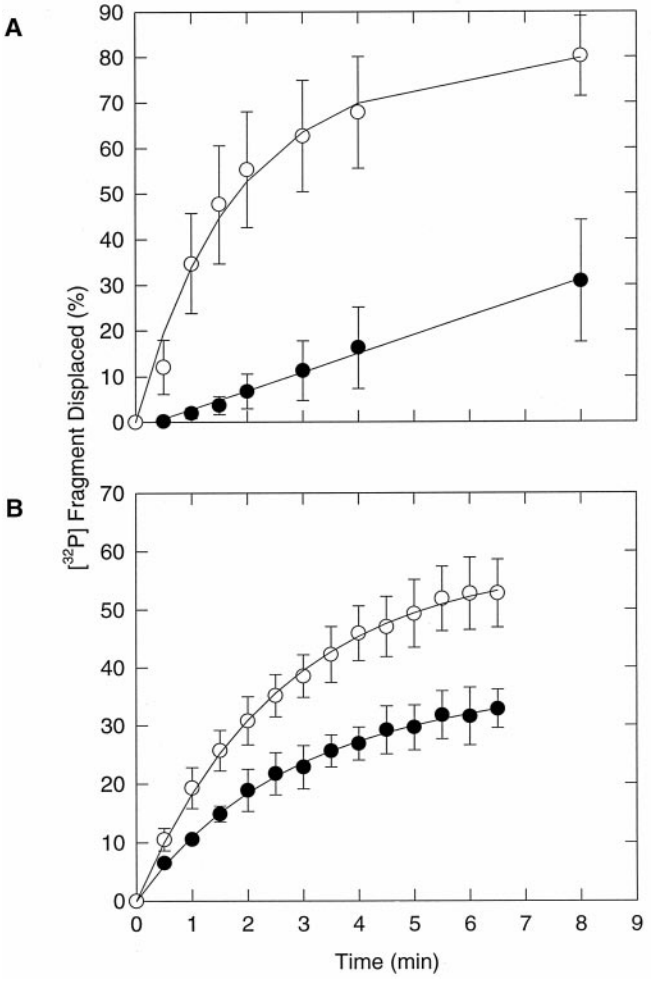

FIG. 4. **Helicase reaction rates for UvrD and UvrD + MutL on long duplex substrates.** The unwinding activity of UvrD (●) or UvrD plus 3.1 nM MutL (○) was measured at the time points indicated as described under "Experimental Procedures." *A*, unwinding of the 750-bp blunt duplex substrate. The concentration of UvrD was 53 nM. *B*, unwinding of the 851-bp partial duplex substrate. The concentration of UvrD was 35 nM. Data represent the average of at least three independent trials. *Error bars* are means ± S.D. The fraction of unwound substrate molecules was calculated for each time point as described (38). *Solid lines* are the curves generated from the fit of equations to data as detailed under "Results."

ing is an early step in the unwinding reaction, a burst of unwinding early in the reaction might be expected in reactions containing both UvrD and MutL, as compared with reactions containing UvrD alone. Therefore, the effect of MutL on the rate of unwinding by UvrD was examined. Long DNA substrates (750-bp blunt duplex and 851-bp partial duplex) were used in this analysis because the regions of DNA excised in mismatch repair can be up to 1 kilobase in length (1, 19).

The extent of unwinding by UvrD was examined at multiple time points in the presence (Fig. 4, *A* and *B*, ○) or absence (●) of 3.1 nM MutL using both substrates. No unwinding was detected with MutL alone (data not shown). Clearly, MutL stimulated the rate of unwinding by UvrD on both the 750-bp blunt duplex (Fig. 4*A*) and 851-bp partial duplex (Fig. 4*B*) substrates. However, the rate enhancement by MutL was substantially greater on the 750-bp blunt duplex substrate than on the 851-bp partial duplex substrate.

The data from both the 750-bp blunt duplex and 851-bp partial duplex substrates were analyzed using Equation 1 as described under "Experimental Procedures." This equation describes unwinding as a biphasic process with a burst phase ($A_b(1 - e^{(-k_b t)})$) and a steady-state phase ($v_{ss}t$). The burst phase of unwinding was due to molecules of UvrD that were preloaded on the DNA substrate prior to initiation of the reaction. The steady-state phase of unwinding, or the observed second phase of the unwinding reaction, was accomplished by those protein molecules that were not preloaded on the DNA substrate or that had fallen off after initiation and then rebound the substrate (41, 45).

The exponential equation did not fit the observed data for unwinding catalyzed by UvrD alone on the 750-bp blunt duplex substrate (Fig. 4*A*, ●). The equation that described the data well was a linear equation representing only the steady-state phase of the unwinding reaction ($v_{ss}t$). The rate of UvrD-catalyzed unwinding of the 750-bp blunt duplex substrate was determined to be 0.21 ± 0.01 fmol of substrate unwound per min (Table I). A similar rate was determined using another substrate preparation (data not shown). Preloading of UvrD onto this substrate was inefficient since only the steady-state phase of the reaction was observed in the absence of MutL. The absence of a detectable burst phase of unwinding by UvrD alone further indicates that even if some molecules of UvrD are

TABLE I
Rate constants for UvrD- and (UvrD + MutL)-catalyzed unwinding on long DNA substrates

Rate constants were calculated from unwinding experiments shown in Fig. 4 as described under "Experimental Procedures." ND, not determined.

Substrate	Protein	A_b [a]	k_b [a]	v_{ss} [a]
		fmol	*min*$^{-1}$	*fmol/min*
750-bp blunt duplex	UvrD	ND	ND	0.21 ± 0.01
	UvrD + MutL	3.98 ± 0.95	0.61 ± 0.20	0.06 ± 0.11
851-bp partial duplex	UvrD	2.26 ± 0.04	0.44 ± 0.08	0.08 ± 0.06
	UvrD + MutL	3.76 ± 0.40	0.45 ± 0.05	0.11 ± 0.06

[a] A_b is the amplitude of the burst phase, k_b is the rate constant for describing the burst phase of the unwinding reaction, and v_{ss} is the rate for the steady-state phase of the unwinding reaction.

preloaded on this substrate, these molecules dissociate before completion of unwinding of the duplex. Therefore, the only unwinding detected is due to unwinding by protein molecules binding from solution after initiation of unwinding, defined as the steady-state phase of the reaction (41).

On the other hand, the unwinding of the 750-bp blunt duplex by UvrD + MutL was well described by two distinct phases (Fig. 4*A*, ○). Therefore, Equation 1 was used to analyze the data from these experiments. A_b, k_b, and v_{ss} were calculated for UvrD-catalyzed unwinding in the presence of MutL (Table I). The calculated values of A_b, k_b, and v_{ss} were 3.98 ± 0.95 fmol, 0.61 ± 0.2 min^{-1}, and 0.06 ± 0.11 fmol min^{-1}, respectively. The rate constants calculated for a second preparation of the 750-bp substrate were nearly identical (data not shown). Interestingly, the steady-state rate of unwinding by UvrD in the presence of MutL (0.06 ± 0.11 fmol min^{-1}) on this substrate was similar to, or within error of, the steady-state rate of unwinding catalyzed by UvrD alone (0.21 ± 0.01 fmol min^{-1}). The slightly lower steady-state rate in the presence of MutL was likely due to the concentration of substrate becoming limiting in the later phase of the reaction because much of the substrate was unwound during the burst phase of the reaction. These data support the notion that the burst in unwinding in the presence of MutL is due to preloading of UvrD and that the steady-state rate reflects unwinding after UvrD has dissociated and rebound to the DNA.

Equation 1 could also be used to describe the data from rate experiments using the 851-bp partial duplex DNA substrate (Fig. 4*B*). Similar results were obtained by fitting the equation for a single exponential process to the data. However, Equation 1 described the data better since the unwinding reaction by UvrD and UvrD in the presence of MutL had two phases. The burst amplitude (A_b) for unwinding catalyzed by UvrD alone was 2.26 ± 0.40 fmol unwound; the rate constant for the burst phase (k_b) was 0.44 ± 0.08 min^{-1}; and the steady-state rate (v_{ss}) was 0.08 ± 0.06 fmol unwound per min (Table I). For the unwinding reaction catalyzed by UvrD in the presence of MutL, A_b was 3.76 ± 0.40 fmol, k_b was 0.45 ± 0.05 min^{-1}, and v_{ss} was 0.11 ± 0.06 fmol min^{-1}. Therefore, on the 851-bp partial duplex substrate, UvrD was able to preload and complete unwinding to produce the exponential phase of unwinding in the absence of MutL. However, the amplitude of the burst phase was greater in the presence of MutL. This result suggests that more molecules of UvrD are preloaded as productive complexes in the presence of MutL. Moreover, the rate constants for the burst phase of unwinding by UvrD and UvrD + MutL were identical. The data analysis indicates that the reason stimulation of unwinding by MutL is more significant on the 750-bp blunt duplex is due to the inability of UvrD, in the absence of MutL, to efficiently load on this substrate. However, UvrD

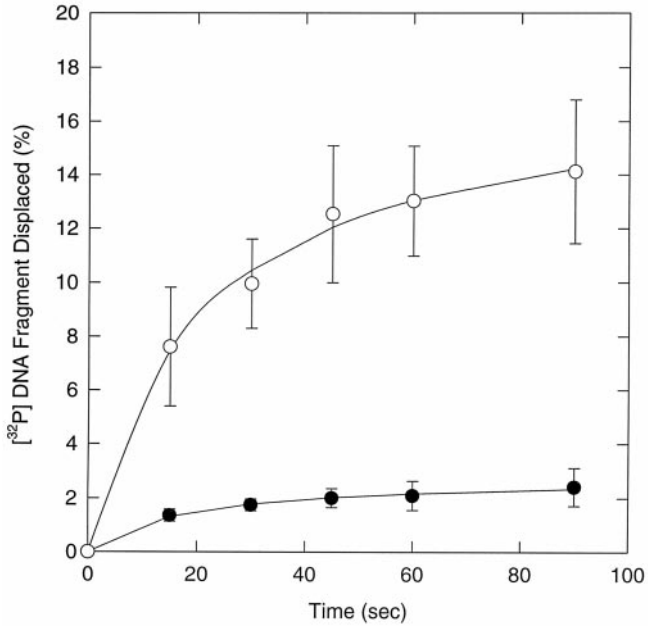

FIG. 5. **Single-turnover unwinding experiments with the 92-bp partial duplex substrate.** The unwinding activity of 20 nM UvrD (●) or 20 nM UvrD plus 20 nM MutL (○) was measured at the time points indicated as described under "Experimental Procedures." Data represent the average of at least three independent trials. *Error bars* are means ± S.D. The fraction of unwound substrate molecules was calculated for each time point as described (38). The equation for a rectangular hyperbola was fit to the data (*solid lines*) using SigmaPlot.

loads efficiently onto the 851-bp base pair partial duplex substrate, and less stimulation by MutL is observed. Nonetheless, there is stimulation of the UvrD-catalyzed unwinding reaction that is likely due to continued loading of UvrD by MutL (see "Discussion"). It should be noted that efficient loading of a helicase, in the absence of any accessory protein such as MutL, has been demonstrated previously to directly increase the burst phase of either UvrD-catalyzed (45) or Rep-catalyzed (41) unwinding. As the protein concentration or the amount of preloaded protein is increased, the rate constant of the burst phase remains constant, whereas the amplitude increases (41, 45).

Single-turnover Unwinding of a 92-bp Partial Duplex—To further address the possibility of continual loading of UvrD by MutL, single-turnover experiments using a 92-bp partial duplex substrate were performed. Since the 92-bp duplex region is beyond the reported processivity of UvrD (40–50 bp) (45), it was expected that when the possibility of continual loading of UvrD onto the DNA substrate was eliminated, less unwinding would be observed than was the case using the 20-bp partial duplex substrate (see Fig. 3). Fig. 5 shows that this is indeed the case; a maximum of 2–3% of the substrate was unwound in the presence of 20 nM UvrD. This reflects both the K_D for binding the substrate and the low probability that a single molecule of UvrD will completely unwind a 92-bp duplex region. In the presence of 20 nM MutL, the fraction of the substrate unwound increased to ~14%, consistent with MutL acting to load more UvrD prior to initiation of unwinding. If MutL were acting as a clamp to increase the processivity of UvrD, then similar fractions of the 20- and 92-bp substrates should be unwound at equivalent concentrations of UvrD and MutL. In addition, since less unwinding by the combination of UvrD and MutL was observed on a 92-bp partial duplex substrate than on the 20-bp partial duplex substrate, continued loading of UvrD by MutL was required for optimal stimulation on this substrate. Moreover, the observation of less unwinding on the 92-bp partial duplex substrate indicates that MutL is not af-

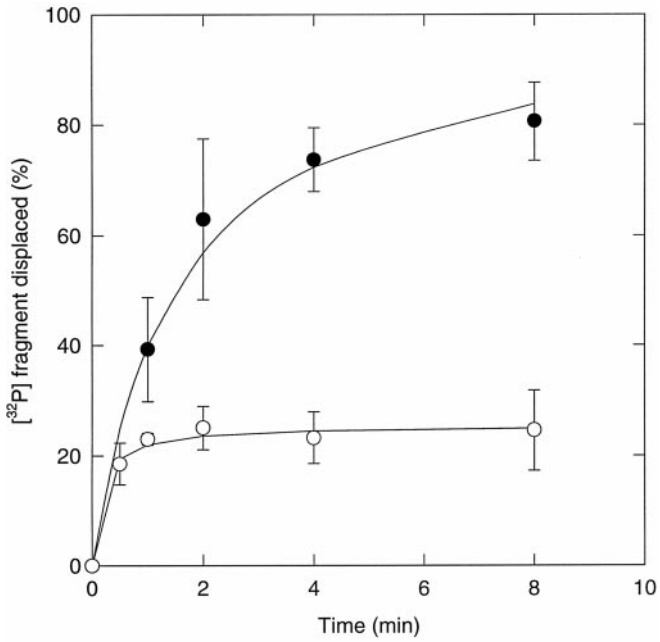

FIG. 6. **Processivity test of UvrD and UvrD + MutL on the 148-bp blunt duplex substrate.** Processivity test experiments were performed as detailed under "Experimental Procedures" for 3 nM UvrD plus 50 nM MutL in the absence of added ssDNA trap (●) or with the addition of the ssDNA trap after 30 s of unwinding (○). Data represent the average of at least three independent trials. *Error bars* are means ± S.D. The fraction of unwound substrate molecules was calculated for each time point as described previously (38). The equation for a rectangular hyperbola was fit to the data (*solid lines*) using SigmaPlot.

fecting the processivity of UvrD. The observed 4-fold stimulation of unwinding on the 92-bp partial duplex substrate is very similar to the 4-fold stimulation caused by the addition of 20 nM MutL to the unwinding reaction involving the 20-bp partial duplex substrate, indicating that the effect of adding MutL is the same with both substrates and most likely reflects a loading phenomenon.

A Test of Processivity with a 148-bp Blunt Duplex—To more directly address the issue of processivity, UvrD (3 nM) and an excess of MutL (50 nM) were incubated with a 148-bp blunt duplex substrate, and unwinding was initiated with ATP. An excess of ssDNA 48-mer trap (4 μM) was added at 30 s to bind free UvrD and to prevent further initiation events. The results of this experiment are shown in Fig. 6. The addition of the trap 30 s after initiation of the unwinding reaction has the effect of completely quenching the reaction. Titration of the trap from 0.4 to 8 μM produced no change in the observed effect (data not shown), indicating that the trap is not acting to actively dissociate UvrD from the DNA. If MutL acted to increase the processivity of UvrD, perhaps by clamping UvrD onto the DNA, the fraction of the substrate unwound would continue to increase after the addition of the ssDNA trap, as UvrD molecules already in the process of unwinding continued to the end of the duplex substrate. However, no increase was observed. In fact, the unwinding reaction ceased immediately, suggesting that additional molecules of UvrD must be loaded to complete unwinding of the 148-bp duplex substrate. This is consistent with the observed low processivity of UvrD (45) and suggests that MutL is not acting as a processivity factor.

DISCUSSION

Both UvrD and MutL are essential components of the *E. coli* mismatch repair machinery (12, 13, 17–19). A physical interaction between these proteins has been demonstrated (25, 27), and MutL greatly stimulates the unwinding activity of UvrD (27, 29). Based on the results presented here, we propose that MutL loads UvrD productively onto the DNA, but does not clamp UvrD onto the DNA during the unwinding reaction. We also suggest that loading of UvrD by MutL is likely to be a continuous process.

The initial indication that MutL acted to load UvrD onto DNA came from DNA binding studies showing that the addition of MutL increased the affinity of UvrD for DNA (data not shown). This prompted an examination of the DNA-binding properties of MutL by nitrocellulose filter binding assays. These studies showed that MutL was able to bind a 92-bp partial duplex DNA in the presence and absence of nucleotide. In contrast, the binding of MutL to ssDNA required the presence of AMP-PNP. MutL binding to ssDNA was significantly reduced when ATP was substituted for AMP-PNP. This likely reflects the higher affinity of MutL for the ATP analog and the fact that a MutL·ATP complex interacts with ssDNA, whereas MutL alone does not interact with ssDNA (21, 24). The DNA binding data reported here are consistent with the most recently reported DNA-binding characteristics of MutL (21).

The binding of UvrD to both ssDNA and partial duplex DNA substrates has been well documented, and it has been shown that the binding affinity of UvrD for ssDNA is increased in the presence of AMP-PNP (see Figs. 1 and 2) (38, 42). The electrophoretic mobility shift assay experiments reported here revealed that UvrD, in the presence of AMP-PNP, formed a weak complex with ssDNA that dissociated during the course of electrophoresis. In the presence of MutL, a supershifted MutL·UvrD·ssDNA complex formed that was more stable than the UvrD·ssDNA complex, suggesting that MutL + UvrD form a specific complex that has a greater affinity for ssDNA than UvrD alone.

Since the DNA binding experiments were equilibrium experiments, it could not be determined from these studies if the MutL-enhanced ssDNA-binding affinity of UvrD was due to an increased rate of association (on-rate) or a decreased rate of dissociation (off-rate) of UvrD with ssDNA. If MutL decreased the UvrD *dissociation* rate, one could envision MutL functioning as a clamp, keeping UvrD tethered to ssDNA as it unwinds and effectively increasing its processivity. Results from unwinding assays using a 148-bp blunt duplex substrate suggested that this was not the case. In these experiments, a ssDNA trap was added after a short period of incubation to effectively prevent reloading of UvrD molecules. Unwinding ceased immediately upon addition of the trap. If MutL were acting to increase the processivity of UvrD, then UvrD already bound to the DNA would continue to unwind the substrate after the addition of the trap to produce an observable increase in unwound product formation. Single-turnover experiments with the 92- and 20-bp partial duplex substrates also indicated that MutL was not acting to increase the processivity of UvrD. A smaller fraction of the 92-bp partial duplex molecules were unwound in comparison with the 20-bp molecules. If MutL were acting to increase the processivity of UvrD, then the same fraction of substrate would be unwound in each case. Moreover, since the degree of stimulation was similar on both partial duplex substrates, stimulation appeared to be independent of substrate length. Taken together, the data described above suggest that a clamping model is improbable.

An increased rate of *association* of UvrD with ssDNA would be reflected in increased loading of UvrD onto the DNA. Preincubation of MutL with UvrD resulted in increased product formation in single-turnover experiments using a 20-bp partial duplex substrate. This stimulation reflects an increase in the amount of productively loaded UvrD. The only unwinding detected under these conditions is due to preloaded UvrD, as

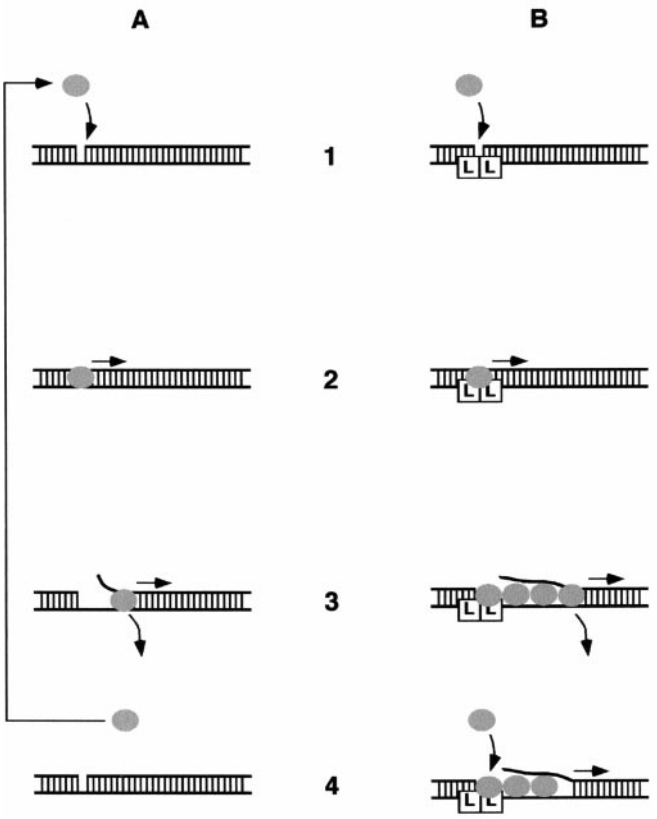

FIG. 7. **Model for the mechanism of UvrD-catalyzed unwinding with the addition of MutL.** The model for unwinding by UvrD (*A*) or UvrD + MutL (*B*) is shown. Details for the model are described under "Discussion." *Step 1* is preloading; *step 2* is with one molecule of UvrD loaded; *step 3* is unwinding; and *step 4* is after dissociation. *Gray ovals* represent UvrD, and *white squares* are MutL (*L*).

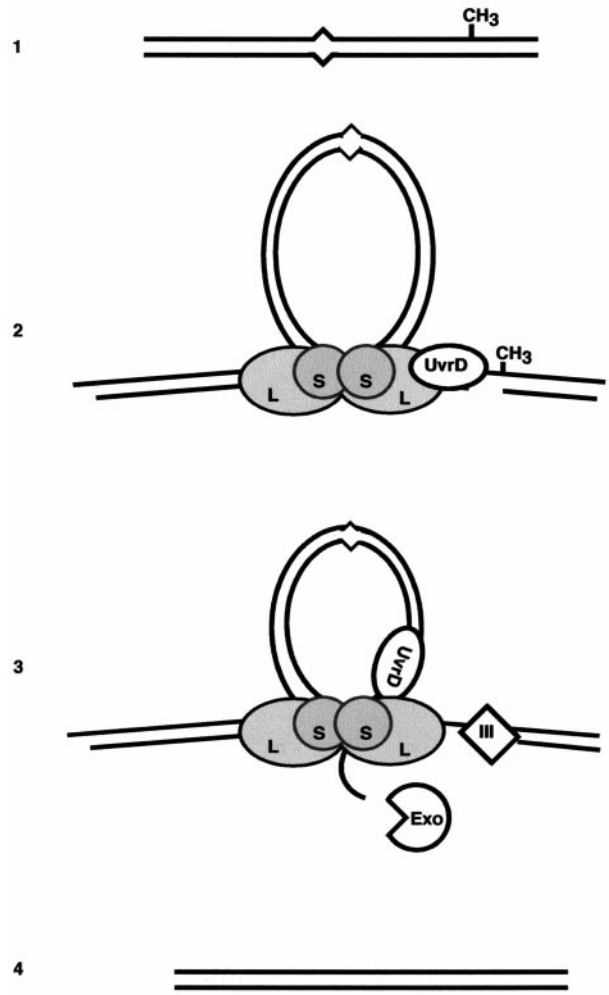

FIG. 8. **Model for *E. coli* mismatch repair.** Details of the mechanism are discussed under "Discussion." Proteins shown in *step 2* are UvrD, MutL (*L*), and MutS (*S*). After unwinding has initiated and the excision step of mismatch repair is progressing (*step 3*), proteins shown are UvrD, MutL, MutS, DNA polymerase III (*III*), and the appropriate single-stranded exonuclease (*Exo*).

shown previously (45). UvrD molecules that fail to bind the DNA or that dissociate from the substrate are trapped by the excess ssDNA. Importantly, as the concentration of MutL was increased, the amplitude of the burst phase increased (see Fig. 3*B*). The concentration at which MutL was half-saturating (40 ± 10 nM) was similar to the K_D for the MutL-partial duplex DNA interaction (~25 nM). We interpret this to indicate that the binding of MutL to DNA is important for its role in stimulating the UvrD-catalyzed unwinding reaction. Thus, two interactions involving MutL are critical for stimulation of the UvrD-catalyzed unwinding reaction: the interaction between MutL and DNA and that between UvrD and MutL.

Increased loading of UvrD by MutL was further investigated using long duplex DNA substrates to model the lengths of DNA substrates likely to be encountered *in vivo*. Data from helicase reactions using a 750-bp blunt duplex or 851-bp partial duplex substrate support the notion that MutL loads UvrD onto DNA and further suggest that loading by MutL is continuous. UvrD-catalyzed DNA unwinding has been characterized as having multiple phases (41, 45, 46). In the data shown here, unwinding of the 750-bp blunt duplex and 851-bp partial duplex substrates was generally described by a burst phase followed by a steady-state phase. The burst phase for these reactions reflects unwinding by those UvrD molecules that were preloaded on the DNA prior to initiation of the reaction by adding ATP, whereas the steady-state phase reflects unwinding by those UvrD molecules (minus MutL) that rebound to the DNA after dissociation. Comparison of the unwinding kinetics exhibited by UvrD on the 750-bp blunt duplex DNA in the presence or absence of MutL clearly showed there was no burst phase in the absence of MutL. This reflects an inability of UvrD to efficiently preload on blunt duplex substrates, as suggested previously (45). The second, or steady-state, phase of the unwinding reaction was similar in the presence and absence of MutL, indicating that MutL does not play a role in this stage of the unwinding reaction. UvrD-catalyzed unwinding of the 851-bp partial duplex substrate was not as dramatically stimulated by the presence of MutL. The major difference in the kinetics of unwinding plus or minus MutL was a slight shift upward in the amplitude during the burst phase of the reaction. This rather small effect of MutL is indicative of the ability of UvrD, in the absence of MutL, to efficiently preload on a substrate that has an excess of ssDNA. Accordingly, ssDNA tails have been reported to facilitate efficient preloading of UvrD (45). The small increase in the amplitude of the reaction suggests that loading of UvrD in the presence of MutL is still more productive than MutL-independent loading on this substrate.

All the data from unwinding assays suggest that more UvrD is productively loaded on the DNA substrate in the presence of MutL. In experiments using the 750-bp blunt duplex and 851-bp partial duplex substrates, the increased productive loading of UvrD is likely to be continuous over the entire course of the unwinding reaction. Considering the reported processiv-

ity for UvrD (40–50 bp) (43), completion of unwinding of these longer substrates and detection of the significant burst phase in the unwinding assay with the 750-bp blunt duplex DNA require multiple binding events by UvrD.

We propose the model shown in Fig. 7 to explain stimulation of UvrD-catalyzed DNA unwinding by MutL. A nicked DNA substrate is shown since this is believed to be the relevant substrate *in vivo*. However, the model is the same for any substrate with a duplex length in excess of the intrinsic processivity of UvrD. The first step (*step 1* to *step 2*) is loading of UvrD onto the DNA. In the presence of MutL (Fig. 7*B*), this rate is enhanced. After it is loaded (*step 2*), UvrD begins to unwind the duplex (*step 3*). In the presence of MutL (Fig. 7*B*), multiple molecules of UvrD are being loaded behind the leading molecule of UvrD. In the absence of MutL, loading of additional UvrD molecules is much slower; and therefore, the concentration of UvrD on the DNA substrate does not increase as rapidly (Fig. 7, *A* (*step 3*) *versus B* (*step 3*)). The high concentration of UvrD increases the overall rate of UvrD-catalyzed unwinding in the presence of MutL. Eventually, the leading molecule of UvrD will dissociate since it is known that UvrD translocates an average of 40–50 bp before dissociating (43). In the case of UvrD alone, the partially unwound duplex can re-anneal when the leading UvrD molecule dissociates, and the whole process must start over (*step 1*). On the other hand, in the presence of MutL, multiple UvrD molecules have been loaded, and the DNA does not re-anneal. The additional UvrD molecules continue the unwinding reaction.

The biological advantage of MutL as an accessory factor that stimulates UvrD-catalyzed unwinding in mismatch repair is clear. Mismatch repair often requires the unwinding of long tracts of DNA (1, 19). Continual loading of UvrD results in an increase in the rate of unwinding. In the absence of MutL, the low processivity of UvrD (43) seems inconsistent with the long repair patch lengths. Therefore, continual loading of UvrD by MutL would increase both the rate and efficiency of the reaction and enable UvrD to unwind the long tracts required in this pathway despite its relatively low intrinsic processivity.

Loading of UvrD by MutL would also explain the ability of UvrD to unwind toward the mismatch. The mismatch repair reaction has bidirectional capability since the hemimethylated d(GATC) site may be located on either side of the mismatch (18). However, UvrD unwinds duplex DNA with a specific polarity (20). Therefore, for UvrD to unwind *toward* the mismatch, it must be loaded on the appropriate DNA strand. If MutL functions to load helicase II onto the DNA, this provides a mechanism to load UvrD exclusively onto the appropriate strand. This would prevent UvrD from unwinding nonspecifically in both directions, as was observed for UvrD-catalyzed unwinding on nicked substrates in the absence of mismatch repair proteins (47, 48).

A model for the role of MutL in *E. coli* mismatch repair is shown in Fig. 8. This model is based on electron microscopic images of MutS and MutL complexes (13) and the data presented here. In *step 1*, a mismatch is recognized by MutS, and a MutS·MutL complex forms a symmetrical loop that increases in size until reaching the nearest hemimethylated d(GATC) site (*step 2*). After nicking by MutH (not shown) and as UvrD unwinds toward the mismatch, the loop structure remains intact. UvrD initiates unwinding at the nick, and UvrD molecules are loaded by MutL. As UvrD unwinds the DNA, the MutS·MutL complex remains bound at the base of the loop structure (*steps 2* and *3*). Consistent with this notion, it was observed that when the complete mismatch repair reaction was included in electron microscopic imaging experiments, MutS and MutL remained bound to the nicked site, and the unwound strand was visualized (13). One of the newly generated single strands (the nicked or nascent strand) is inserted through a groove in the MutL structure (*steps 3* and *4*). A groove has been suggested to function in ssDNA binding by MutL, and double-stranded DNA will not fit within the groove (21). The strand that is being pushed through the groove of MutL is then hydrolyzed by the appropriate exonuclease. The intact ssDNA serves as a template for DNA polymerase III (*step 3*). As the DNA is unwound and pushed through MutL, the loop decreases in size until UvrD reaches the mismatch, providing a possible mechanism for UvrD to "know" when to terminate unwinding. Once UvrD reaches the mismatch, the loop may have decreased to a size that creates torsional strain, forcing the protein·DNA complex to dissociate. Alternatively, a physical interaction between proteins could act as a signal for dissociation. In this model, MutL remains in a constant position with respect to the advancing ssDNA/double-stranded DNA junction and acts catalytically, continually loading UvrD molecules.

MutL is likely to be the master coordinator in the mismatch repair reaction. The interaction of MutL with the three mismatch repair proteins (MutS, MutH, and UvrD) and with DNA is likely to be critical for the proper three-dimensional arrangement of these proteins as well as for the appropriate sequential timing for each event in the repair reaction. Precisely how MutL accomplishes these goals remains to be elucidated. However, the results reported here begin to explain the mechanism by which MutL stimulates UvrD-catalyzed DNA unwinding and demonstrate the importance of MutL binding to DNA.

Acknowledgments—We thank Drs. Dorothy Erie and Mark Hall for advice regarding data interpretation. We also thank Susan Whitfield for help in the preparation of figures and Wolfgang Resch for preparing Fig. 7.

REFERENCES

1. Modrich, P. (1991) *Annu. Rev. Genet.* **25,** 229–253
2. Modrich, P. (1994) *Science* **266,** 1959–1960
3. Modrich, P., and Lahue, R. (1996) *Annu. Rev. Biochem.* **65,** 101–133
4. Rayssiguier, C., Thaler, D. S., and Radman, M. (1989) *Nature* **342,** 396–401
5. Worth, L. J., Clark, S., Radman, M., and Modrich, P. (1994) *Proc. Natl. Acad. Sci. U. S. A.* **91,** 3238–3241
6. Eshleman, J. R., and Markowitz, S. D. (1995) *Curr. Opin. Oncol.* **7,** 83–89
7. Jiricny, J. (1996) *Cancer. Surv.* **28,** 47–68
8. Karran, P., and Bignami, M. (1994) *Bioessays* **16,** 833–839
9. Umar, A., and Kunkel, T. A. (1996) *Eur. J. Biochem.* **238,** 297–307
10. Su, S.-S., Lahue, R. S., Au, K. G., and Modrich, P. (1988) *J. Biol. Chem.* **263,** 6829–6835
11. Su, S.-S., and Modrich, P. (1986) *Proc. Natl. Acad. Sci. U. S. A.* **83,** 5057–5061
12. Grilley, M., Welsh, K. M., Su, S.-S., and Modrich, P. (1989) *J. Biol. Chem.* **264,** 1000–1004
13. Allen, D. J., Makhov, A., Grilley, M., Taylor, J., Thresher, R., Modrich, P., and Griffith, J. D. (1997) *EMBO J.* **16,** 4467–4476
14. Au, K. G., Welsh, K. M., and Modrich, P. (1992) *J. Biol. Chem.* **267,** 12142–12148
15. Modrich, P. (1987) *Annu. Rev. Biochem.* **56,** 435–466
16. Welsh, K. M., Lu, A. L., Clark, S., and Modrich, P. (1987) *J. Biol. Chem.* **262,** 15624–15629
17. Cooper, D. L., Lahue, R. S., and Modrich, P. (1993) *J. Biol. Chem.* **268,** 11823–11829
18. Grilley, M., Griffith, J., and Modrich, P. (1993) *J. Biol. Chem.* **268,** 11830–11837
19. Lahue, R. S., Au, K. G., and Modrich, P. (1989) *Science* **245,** 160–164
20. Matson, S. W. (1986) *J. Biol. Chem.* **261,** 10169–10175
21. Ban, C., Junop, M., and Yang, W. (1999) *Cell* **97,** 85–97
22. Bende, S. M., and Grafstrom, R. H. (1991) *Nucleic Acids Res.* **19,** 1549–1555
23. Drotschmann, K., Aronshtam, A., Fritz, H. J., and Marinus, M. G. (1998) *Nucleic Acids Res.* **26,** 948–953
24. Ban, C., and Yang, W. (1998) *Cell* **95,** 541–552
25. Spampinato, C., and Modrich, P. (2000) *J. Biol. Chem.* **275,** 9863–9869
26. Hall, M. C., Jordan, J. R., and Matson, S. W. (1998) *EMBO J.* **17,** 1535–1541
27. Hall, M. H. (1998) *Escherichia coli DNA Helicase II: Structure-function Analysis of Conserved Amino Acid Motifs and Investigation of Protein-Protein Interactions.* Ph.D. thesis, University of North Carolina, Chapel Hill
28. Hall, M. C., and Matson, S. W. (1999) *J. Biol. Chem.* **274,** 1306–1312
29. Yamaguchi, M., Dao, V., and Modrich, P. (1998) *J. Biol. Chem.* **273,** 9197–9201
30. Sancar, A., and Hearst, J. E. (1993) *Science* **259,** 1415–1420
31. Dao, V., and Modrich, P. (1998) *J. Biol. Chem.* **273,** 9202–9207
32. Lechner, R. L., and Richardson, C. C. (1983) *J. Biol. Chem.* **258,** 11185–11196
33. George, J. W., Brosh, R. M., Jr., and Matson, S. W. (1994) *J. Mol. Biol.* **235,** 424–435

34. Mechanic, L. E., Hall, M. C., and Matson, S. W. (1999) *J. Biol. Chem.* **274,** 12488–12498
35. Runyon, G. T., Wong, I., and Lohman, T. M. (1993) *Biochemistry* **32,** 602–612
36. Brosh, R. M., Jr., and Matson, S. W. (1995) *J. Bacteriol.* **177,** 5612–5621
37. Ausubel, F. M., Brent, R., Kingston, R. E., Moore, D. D., Seidman, J. G., Smith, J. A., and Struhl, K. (eds) (2000) *Current Protocols in Molecular Biology*, pp. 3.4.10–3.4.11, John Wiley & Sons, Inc., New York
38. Hall, M. C., Ozsoy, A. Z., and Matson, S. W. (1998) *J. Mol. Biol.* **277,** 257–271
39. Matson, S. W., and Richardson, C. C. (1985) *J. Biol. Chem.* **260,** 2281–2287
40. Wong, I., and Lohman, T. M. (1993) *Proc. Natl. Acad. Sci. U. S. A.* **90,** 5428–5432
41. Amaratunga, M., and Lohman, T. M. (1993) *Biochemistry* **32,** 6815–6820
42. Mechanic, L. E., Latta, M. E., and Matson, S. W. (1999) *J. Bacteriol.* **181,** 2519–2526
43. Ali, J. A., and Lohman, T. M. (1997) *Science* **275,** 377–380
44. Brosh, R. M., Jr., and Matson, S. W. (1996) *J. Biol. Chem.* **271,** 25360–25368
45. Ali, J. A., Maluf, N. K., and Lohman, T. M. (1999) *J. Mol. Biol.* **293,** 815–834
46. Bjornson, K. P., Amaratunga, M., Moore, K. J., and Lohman, T. M. (1994) *Biochemistry* **33,** 14306–14316
47. Runyon, G. T., Bear, D. G., and Lohman, T. M. (1990) *Proc. Natl. Acad. Sci. U. S. A.* **87,** 6383–6387
48. Runyon, G. T., and Lohman, T. M. (1989) *J. Biol. Chem.* **264,** 17502–17512